Bulletin of the New Zealand Society for Earthquake Engineering, Vol. 51, No. 2, March 2018

THE IMPLICATIONS OF POST-TENSIONING LOSSES ON THE SEISMIC RESPONSE OF PRES-LAM FRAMES

Gabriele Granello[1], Alessandro Palermo[2], Stefano Pampanin[3], Tobias Smith[4] and Francesco Sarti[5]

(Submitted *March 2017*; Reviewed *June 2017*; Accepted *July 2017*)

ABSTRACT

Since 2010, twelve post-tensioned timber (Pres-Lam) buildings have been constructed throughout the world. In high seismic areas, Pres-Lam technology typically combines unbonded post-tensioning tendons and supplemental damping devices to provide moment capacity to beam-column, wall-foundation or column-foundation connections. Over time creep within the timber elements leads to losses in post-tensioning forces reducing the connection moment capacity. This paper analyses how different post-tensioning loss scenarios, depending on the beam-column joint detailing, impact the building's seismic response. Two case study buildings were designed and investigated using the Acceleration-Displacement Response Spectrum (ADRS) method and Non-Linear Time History Analysis (NLTHA) to predict seismic performance. These buildings were considered to be located in areas of high and low seismic risk, leading to designs with and without the use of damping devices, respectively. The results show that the building with additional damping responded with similar peak displacements, even under extreme loss scenarios. In comparison, when supplemental damping was not used, peak displacements increased significantly with post-tensioning losses.

INTRODUCTION

The Precast Seismic Structural System (PRESSS) program [2, 3] was an extensive project carried out in the 1990s and coordinated by the University of California, San Diego. Among the different connections developed and tested, the program showed that the hybrid connection proved to be an efficient low-damage solution for precast concrete buildings. The hybrid connection combines unbonded post-tensioning tendons and mild steel bars and allows the accommodation of high seismic demand through controlled rocking between structural elements. While tendons provide re-centering capability to the system, supplemental damping allows for hysteretic energy release as well as providing additional moment capacity. These damping devices can be internal or external to the connection. However, when they are externally placed, they have the additional advantage of being replaceable.

In 2002, the hybrid concept was extended to steel members [4] which provided support to the idea that the hybrid connection is material independent. In 2005, the technology was extended to engineered timber products at the University of Canterbury [5, 6] and referred to as the Pres-Lam system. Extensive laboratory testing in New Zealand [7-11] and overseas [12] has proven the connection to have good seismic performance, which was characterized by no residual displacements, negligible structural damage in the timber members, and stable, non-degrading hysteretic response. An analytical design procedure was developed to be able to accurately predict elastic and inelastic performance under horizontal and gravity loading, and numerical models have been developed to assist in the reproduction and prediction of total building response [13].

While an extensive and comprehensive body of research was completed, a gap still exists regarding the quantification and understanding of the impact of post-tensioning losses. This means that as designers have been adopting Pres-Lam, conservative assumptions have had to be made, which in some cases has complicated detailing.

It is widely accepted and logical that post-tensioning loss derived from creep phenomena in compressed timber members will lead to a reduction of the connection moment capacity. Experimental and analytical studies [14-16] have suggested that expected losses are in the range of 6-50% in 50 years for most practical cases mainly depending on the load direction (6-10% if timber is loaded only parallel to the grain, but up to 50% if timber is loaded perpendicular to the grain). Frame structures are therefore more likely to sustain post-tensioning losses than wall or column systems; hence, efforts have focused on the reinforcement of the beam-column joint. Different detailing solutions include the use of steel plates, screws, or rods (Figure 1b, c, d), or rotated timber panels (Figure 1a). The use of hardwood columns made of ash were also proposed [17] and implemented in the ETH House of Natural Resources (Figure 1e) [18].

This paper shows the numerical study of the seismic response of two case study Pres-Lam frame buildings. The two structures are placed in high and low seismic areas respectively. Additional damping is provided to the first building through the attachment of external mild steel dissipation devices, whereas the second one is only post-tensioned. It is conceivable that in low seismic risk areas that a designer may choose not to include external dissipaters.

The seismic response of the frames in case of frequent (1 in 25 years) or rare (1 in 500 year) events is assessed through the use of Acceleration-Displacement Response Spectra (ADRS) and Non-Linear Time History (NLTH) analyses. The key indicators of displacement demand, total base shear, and hysteretic damping are presented, and the design implications are then discussed. Post-event residual displacements, a key factor in building reparability, are also assessed.

[1] *Corresponding Author, Lecturer, University of Canterbury, Christchurch, gabriele.granello@canterbury.ac.nz (Member)*
[2] *Professor, University of Canterbury, Christchurch, alessandro.palermo@canterbury.ac.nz (Member)*
[3] *Professor, University of Canterbury, Christchurch; Professor, Sapienza University of Rome, Italy, stefano.pampanin@canterbury.ac.nz (Fellow)*
[4] *Structural Engineer, PTL Consultants, Christchurch, t.smith@ptlnz.com (Member)*
[5] *Structural Engineer, PTL Consultants, Christchurch, f.sarti@ptlnz.com (Member)*

Figure 1: Operative post-tensioned timber buildings: a) Massey University, Wellington (courtesy of Andy Buchanan); b) Trimble Office, Christchurch (courtesy of Paul Drummond); c),d) Merritt Building, Christchurch (courtesy of Andy Buchanan); e) ETH House of Natural Resources, Zurich (Copyright ETH Zurich).

Likely Post-tensioning Losses of Pres-lam Buildings

Since this paper investigates how post-tensioning losses can affect the overall building performance, some assumptions on the likely losses have been made. These likely losses are based on the results monitored on operative structures presented below.

The Trimble Navigation Office (Figure 1b) was constructed in Christchurch (New Zealand) following the Canterbury Earthquakes of 2010 and 2011 [19] using Pres-Lam walls and Pres-Lam frames in each orthogonal direction. The two storey frames made of LVL are horizontally post-tensioned only at the first floor level with no post-tensioning being placed at roof level. External steel reinforcing is used at both levels to protect the columns (Figure 2a) and to anchor replaceable 'plug and play' energy dissipaters [20].

The structure is currently under monitoring by a comprehensive system of measurement [21, 22] including accelerometers to measure floor accelerations during a seismic event, load cells to measure post-tensioning forces in both the frames and walls, and several strain gauges to measure the strain levels of the external dissipaters.

Post-tensioning force ratios (measured post-tensioning force over initial post-tensioning force) are shown in Figure 2b for the three frames being monitored. It can be seen the average post-tensioning loss is less than 5% in approximately two years, resulting in an expected loss of 25-30% in 50 years [23]. The smaller loss (compared to the EXPAN Building in Figure 4) is due to the beam-column detailing where the steel plates in fact reduce the amount of creep occurring in the column.

The House of Natural Resources (Figure 1e) [18] in Zurich (Switzerland) also contains Pres-Lam frames with continuous measurement of post-tensioning force.

The lateral load resisting system consists of post-tensioned Glulam frames in both directions with spruce beams and ash columns. The use of hardwood in the columns (Figure 3a) is proposed due to its superior long-term performance perpendicular to the grain. As the building is located in a low-seismic area, no supplemental damping devices were adopted.

The structure is fully instrumented [24] with several accelerometers on each floor level, load cells in correspondence of the tendons, and moisture probes to measure the moisture content in the timber elements.

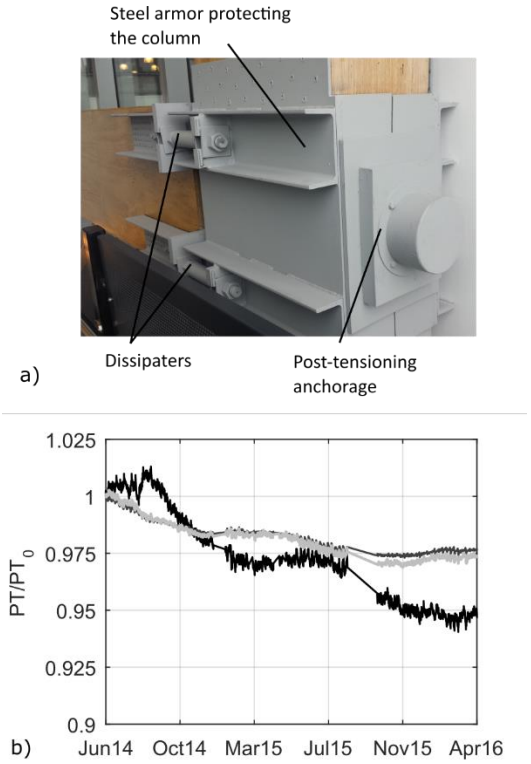

Figure 2: Trimble Navigation Office: a) beam-column detailing (Courtesy of Paul Drummond) and b) post-tensioning forces under monitoring in the frame [22].

Post-tensioning force ratios are reported in Figure 3b [24], which shows an average amount of less than 5% in one year and two months. This would result in an expected post-tensioning loss of 15-20% in 50 years [23]. These preliminary results suggest that the use of hardwood in the beam-column joint panel is a viable solution to mitigate post-tensioning loss.

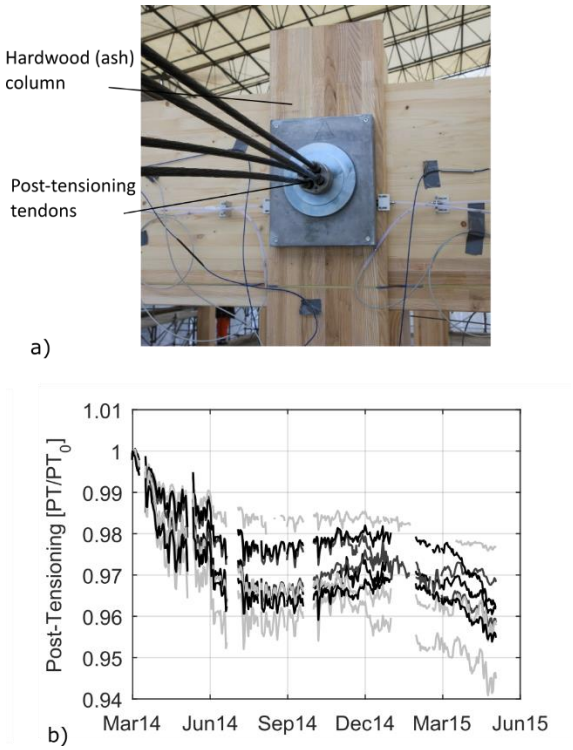

Figure 3: House of Natural Resources: a) Joint detailing (Copyright ETH Zurich) and b) Post-tensioning trend over time [24].

Finally, the University of Canterbury Expan building (Figure 4a) was originally a test specimen used in the University's laboratories [25]. After the testing programme, the building was dismantled and re-erected as the head office of the Structural Timber Innovation Company (STIC) [26].

The two-storey building consisted of lateral resisting post-tensioned timber frames in the longitudinal direction and post-tensioned coupled shear walls in the opposite direction. Due to the low seismic mass, the connections were purely post-tensioned without any dissipation devices.

While the beam-column joint panels at the first level were reinforced to avoid stressing the joint panel area, the roof level joint panels were intentionally left unprotected, representing the extreme case of potential post-tensioning loss.

Laser measurements of the frame length were carried out [27], and estimated post-tensioning losses are shown in Figure 4b. It shows that over a two-year period, post-tensioning losses as high as 80% were estimated in the Pres-lam frames with unreinforced joint panels, while a 10-15% was estimated with joint panel reinforcement. While these loss values are not based on accurate instrumentation readings, they highlight that post-tensioning losses can be significant when a column is simply left to transfer the post-tensioning load.

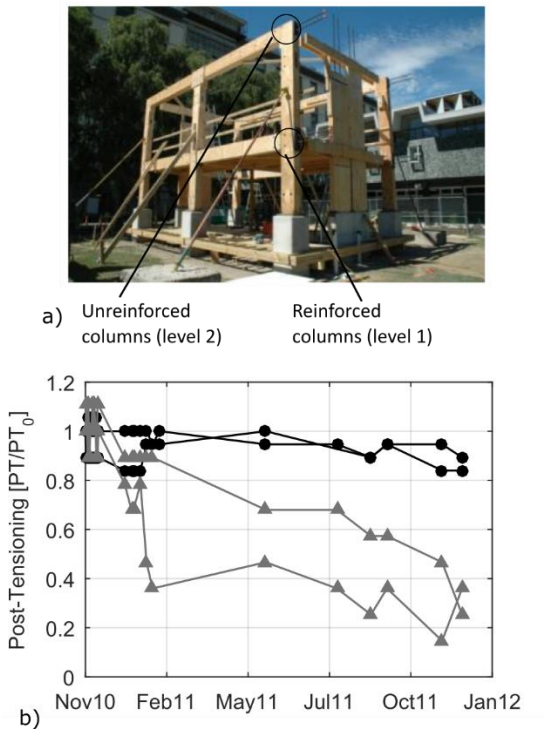

Figure 4: Expan Building: a) view during construction [26] and b) post-tensioning trend over time for the top floor (grey line) and bottom floor (black line)[27].

In conclusion, the expected post-tensioning loss in a well detailed building is less than 20% for a beam-column joint with hardwood (labelled as joint type A e.g. House of Natural Resources) and less than 30% for the beam-column joint with steel plates (labelled as joint type B e.g. Trimble) in 50 years [23]. Although not recommended, extreme scenarios for poor detailed solutions (e.g. Expan Building-level 2, labelled joint solution C) of up to 90% of loss will be discussed in this paper. A summary of losses is presented in Table 1.

Table 1: Post-tensioning losses considered at 50 years for different joint detailing.

Joint Label	Reinforcement Type	Likely Loss at 50 Years
A	Ash	20%
B	Steel Plates	30%
C	-	90%

CASE STUDY BUILDING

The two four-storey case study buildings were designed with a lightweight timber penthouse at the top floor (Figure 5). Each floor was selected to be 32 × 19.5 m in plan with a total floor area of 624 m^2 (Figure 6). The case study building was assumed to be located in two different seismic areas: a high seismic zone (Z=0.3 e.g. Christchurch, New Zealand) and low-medium seismic zone (Z=0.18 e.g. New Plymouth, New Zealand). Both structures were considered to be situated on soft or deep soils (soil type D according to the New Zealand Standard 1170.5 at 3.1.3).

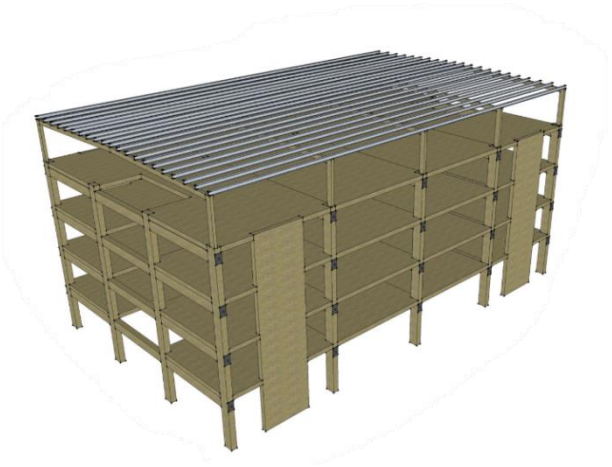

Figure 5: Render of the case study Building.

The structural systems used in the case study buildings were Pres-Lam frames in the transverse direction and Pres-Lam walls in the longitudinal direction. A building live load of 3 kPa (i.e. office use NZS 1701.1 at 3.4.1) was assumed to act on a floor system made up of 21 mm thick plywood panels on top of 90 x 400 mm timber joist at 0.6 m without any concrete. As mentioned above, post-tensioning losses are more likely to occur in frame structures, therefore these were the focus of the study.

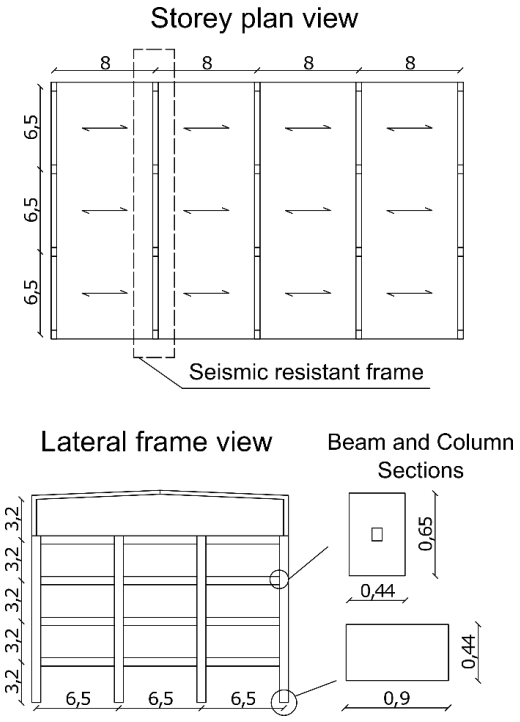

Figure 6: Storey plan view and lateral frame view of the case study building.

Beam and column dimensions of 650 x 441 mm 900 x 441 mm respectively were required to satisfy an inter-storey drift limit equal to H/300 (i.e. 0.33%) for likely events with a return period equal to 25 years. A summary of the seismic masses is reported in Table 2.

The connection (detailing in Figure 7) with the addition of the 'plug and play' dissipation devices was designed to target a design re-centring ratio, β, (defined as the ratio between post-tensioning moment and the total moment capacity) of 0.7. Seven wire strands were used as the post-tensioning elements.

Table 2: Seismic masses acting on the frame.

Seismic masses			
Floor	**[KN]**	**[KN]/frame**	**[KN]/wall**
4	3130	626	782
3	3193	639	798
2	3193	639	798
1	3193	639	798
Tot	12710	2542	2542

While post-tensioning tendons are positioned at the section centroid of the beam section, dissipaters are placed ± 250 mm from the beam centreline. Material properties for timber members LVL grade 16, post-tensioning steel, and mild steel are reported in Table 3, Table 4, and Table 5 respectively.

*Table 3: LVL Grade 16 properties: f_b bending strength, $f_{c,par}$ compression strength parallel to the grain, $f_{c,perp}$ compression strength perpendicular to the grain, f_s shear strength, E_{par} elastic modulus parallel to the grain, E_{perp} elastic modulus perpendicular to the grain (*assumed), G shear modulus.*

f_b [MPa]	$f_{c,par}$ [MPa]	$f_{c,perp}$ [MPa]	fs [MPa]	E_{par} [GPa]	E_{perp} [GPa]	G [GPa]
65	48	12	4.6	16	0.55*	0.8

Table 4: Steel tendon properties: φ_i tendon diameter, A_{pi} tendon area, f_{ptk} ultimate stress, f_{pt01k} nominal yielding stress and E elastic modulus.

φ_i [mm]	A_{pi} [mm^2]	f_{ptk} [MPa]	f_{pt01k} [MPa]	E [GPa]
12.7	100.1	1860	1674	195

Table 5: Mild steel properties respectively: f_y yielding stress, f_u ultimate stress, E_s elastic modulus, ε_y yielding strain, r post-yielding stiffness ration.

f_y [MPa]	f_u [MPa]	E_s [MPa]	ε_y [-]	r [-]
300	420	200	0.0015	0.008

Column and beam sections were governed by serviceability requirements (i.e SLS drift limit). A summary of post-tensioning and mild steel layout is presented in Table 6.

Table 6: Post-tensioned connection detailing with and without additional damping.

	Storey	Tendons number	Post-tensioning [KN]	Tendons Stress [%f_{pt01k}]	Mild Steel
With Dissipaters	1&2	3	300	60%	4φ12
	3&4	2	200	60%	4φ10
Without Dissipaters	1&2	2	200	60%	-
	3&4	2	200	60%	-

A semi-rigid moment connection (detailing in Figure 7) was designed at the column-foundation level. Analysis showed that despite satisfactory performance being obtained for strong and rare events (e.g. return period equal to 500 years), drift limits (often controlled by non-structural damage) were exceeded in the case of less intense but more likely (e.g. return period equal 25 years) earthquakes. This required a stiff connection to be introduced to limit first floor drift.

The possibility of introducing external dissipaters, which would be easier to replace, was also explored. However, this solution was not feasible due to the high number of connectors necessary between the dissipaters and the column. Shear keys were also provided for transferring shear and avoiding the internal bars working in dowel action.

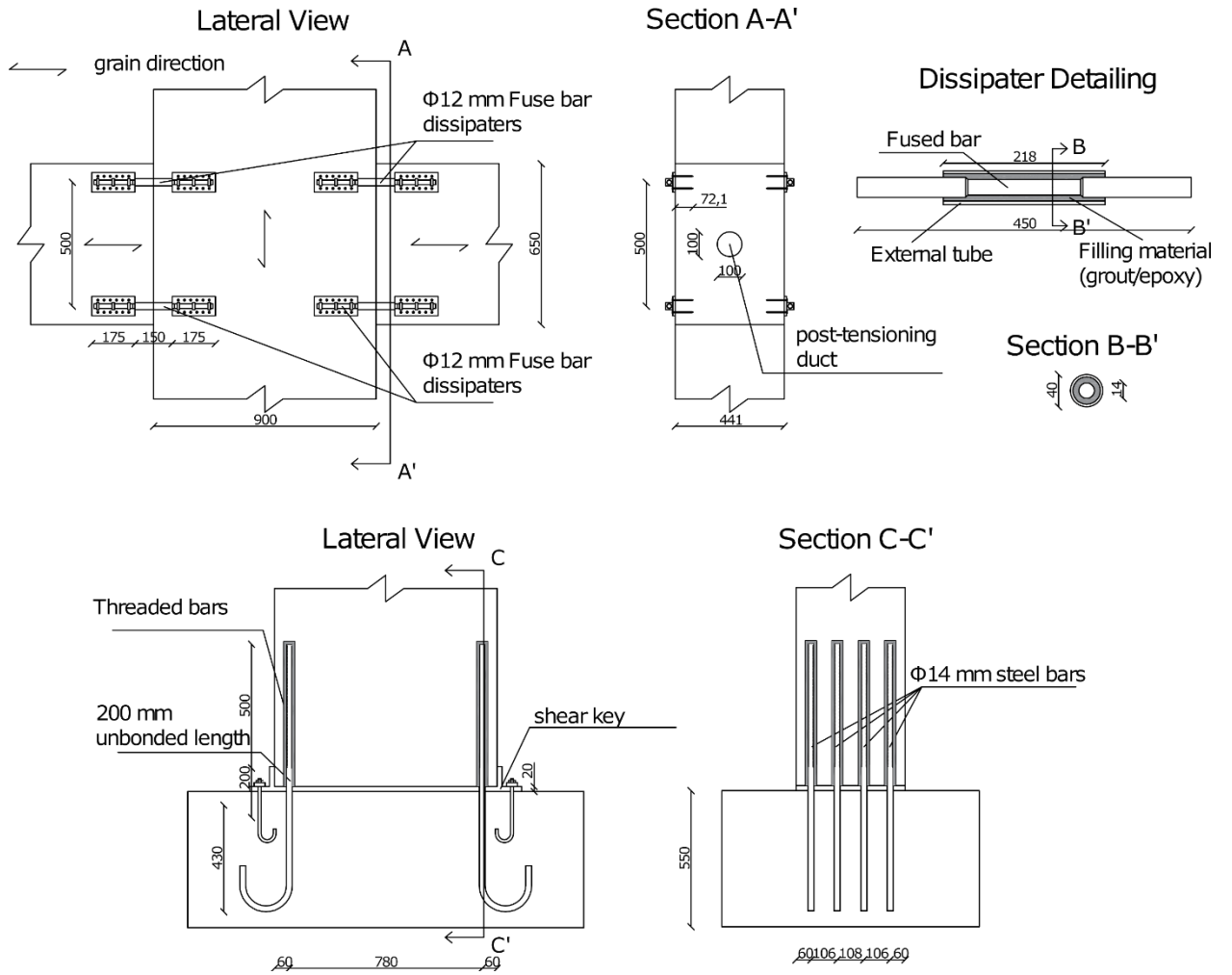

Figure 7: Structural detailing: beam-column hybrid joint, column-base joint and fuse dissipater.

Push-pull Connection Analysis

The moment-rotation behaviour of a post-tensioned timber connection was defined using an iterative analytical procedure developed by Palermo [28] , extended to the Pres-lam system by Newcombe et al. [29], and further developed by Smith [30]. This last approach in particular showed to adequately (with limited error) predict the behaviour of post-tensioned timber frames.

Lumped plasticity models (see Figure 8) were then calibrated against the moment-rotation response using rotational springs in parallel and in series: (i) a multi-linear elastic hysteresis for the post-tensioning contribution, (ii) an elasto-plastic rule for the mild steel contribution and (iii) an elastic-rigid rule for the internal rotation before the gap opening contribution. An additional rotational spring was placed at the beam-column joint to take into account the joint shear stiffness [30].

Depending on environmental conditions and joint detailing, a well-designed building is expected to not exceed 30% of post-tensioning loss in 50 years (see Section: Likely Post-tensioning Losses of Pres-lam Buildings). However, losses greater than 50% can occur if timber (excluded hardwood) is directly loaded perpendicular to the grain (as in the case of the Expan Building).

In this study, different post-tensioning loss scenarios equal to 20% (joint type A), 30% (joint type B) and 90% (joint type C) were considered, and the seismic response was compared with the initial condition.

The post-tensioning loss influence on the hybrid connection behaviour is shown in Figure 9 for both the post-tensioning contribution (Figure 9a) and the global response (Figure 9b). At this stage, the modelling is limited to the joint response. The moment rotation contribution given by steel is not reported as independent with respect to post-tensioning loss.

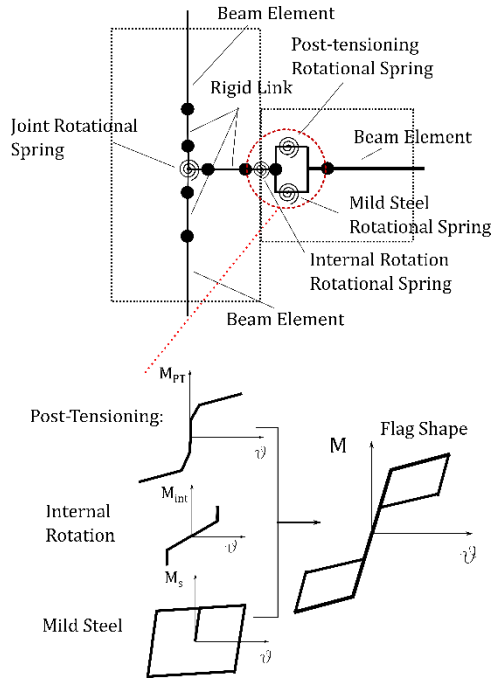

Figure 8: Post-tensioned timber connection modelling.

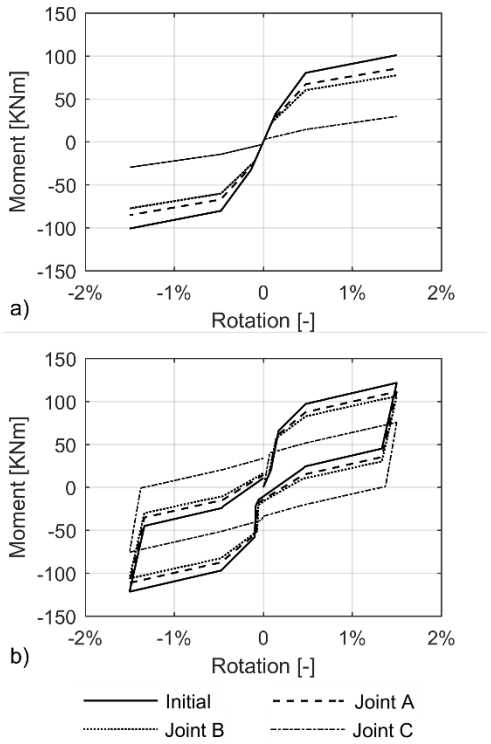

Figure 9: Moment rotation behaviour for different levels of post-tensioning loss: a) post-tensioning contribution and b) overall response.

In general, four main effects can be observed with increasing post-tensioning loss:

1. The decrease of the decompression moment, i.e. the point at which the gap opens - The decompression point is reached when the compression stress drops to zero in the extreme fibre of the beam section. As the decompression moment is directly proportional to the axial load applied to the section, any post-tensioning loss results in the opening of the gap at a lower moment demand.
2. Lower total connection maximum capacity - As the moment capacity contribution given by post-tensioning is reduced, the total capacity is also reduced.
3. Increased residual rotation resulting from the loss of re-centring capacity - If post-tensioning decreases, its contribution to the moment capacity decreases as well. If the re-centring ratio, β, drops below 0.5, the connection loses its re-centring capability leading to significant residual deformations.
4. Increase of area within the moment-rotation loop - As the decompression moment is anticipated, dissipaters are engaged at a lower level of rotation.

The observations above were noted from the static analysis of a single beam column joint, and do not provide an exhaustive indication of the global behaviour. Therefore, the following sections further investigate the dynamic behaviour of the buildings through ADRS and NLTH analyses.

Acceleration Displacement Response Spectra (ADRS) Analysis

An ADRS analysis [31] was carried out in order to evaluate the global performance of the prototype frames for seismic events with 25 and 500 year return periods corresponding to Service Limit State (SLS) and Ultimate Limit State (ULS).

Pushover curves were evaluated for both structures using the analysis software OpenSEES [32]. In the analysis, a triangular force distribution was used as a representation of seismic loading in accordance to NZS 1170.5 at 6.2.1.3. The connection behaviour was simulated as described above with all other timber members being represented as elastic elements. The force-displacement pushover curve was then converted into an equivalent single degree of freedom acceleration-displacement plot [31].

The curves were bi-linearized to estimate the nominal ductility by considering the initial tangent stiffness and the energy (area between the curve and the x axis) necessary to reach the 2.5% drift displacement at the last floor as shown in Figure 10. The change of stiffness point was considered as nominal yielding displacement and indicated with d_y.

It is worth noting that dissipaters are not activated exactly in correspondence of d_y: as the pushover is approximated by a bilinear curve, a slight difference may exist, and this may introduce a slight overestimation of damping.

The 5% design spectrum was then reduced considering the damping characteristics of the system. For post-tensioned rocking structures, the hysteretic damping $\xi_{hyst,str}$ can be expressed according to Equation 1[33]:

$$\xi_{hyst,str} = \frac{(2-2\beta)(\mu-1)}{\mu\pi(1+r(\mu-1))} \quad (1)$$

where μ is the structural ductility factor, β the global re-cantering ratio, and r the post-yield stiffness ratio equal to 0.8%. The equivalent viscous damping ξ is the sum of the elastic damping, ξ_{el}, and the hysteretic damping (reduced by 70% [30]):

$$\xi = \xi_{el} + \xi_{hyst,str} \quad (2)$$

The equivalent viscous damping, ξ, was then used to calculate the spectral reduction factor R_ξ as:

$$R_\xi = \sqrt{7/(2+\xi)} \quad (3)$$

When additional dissipation is not provided, the 5% design spectrum was considered, i.e. R_ξ=1.

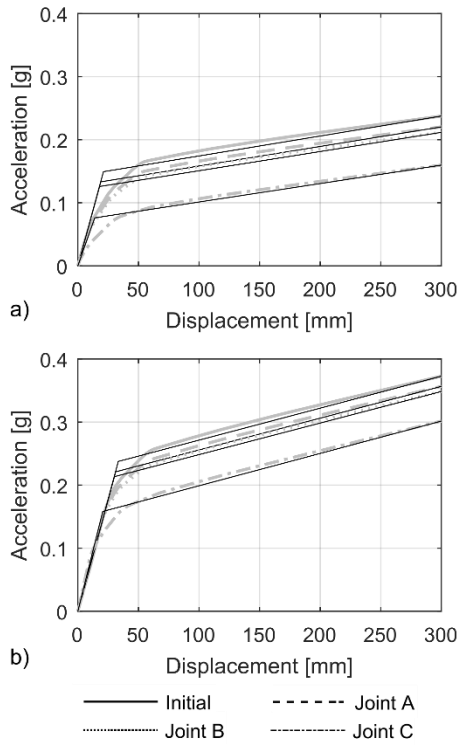

Figure 10: Acceleration-displacement curves respectively for a) the building without additional damping and b) with additional damping.

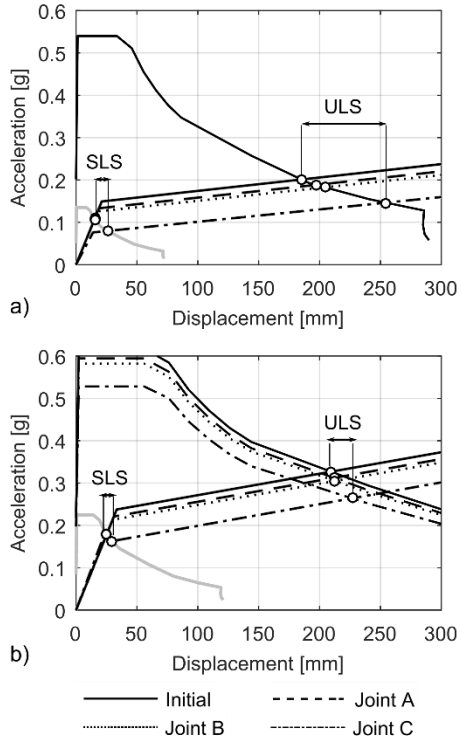

Figure 11: Acceleration Displacement Response Spectra (ADRS) analysis respectively for the a) building without and b) with dissipaters.

The intersection between the bi-linearized Acceleration-Displacement curves and the (damped) spectra is reported in Figure 11.

The nominal yielding displacement, d_y, the intersection displacement, d_i, and the spectral acceleration, a_i, the ductility, μ, (expressed as ratio between the intersection displacement over the nominal yielding displacement), damping, ξ, maximum drift, dr_i, increment of drift respect to the initial condition $\Delta\, dr_i$, and maximum strain in the dissipaters , ε_{diss}, at the performance point (i.e the intersection of the push-over and the equivalent SDOF acceleration-displacement curves) are reported in Table 7.

For a frequent earthquake (return period equal 25 years), both structures remain within their primary linear elastic range (interstorey drift < 0.33%) when post-tensioning loss are within 30% (i.e. all the details solutions but Joint C). In other words, the moment demand induced by the ground motions does not overcome the decompression moment, and therefore the rocking motion is not triggered.

When post-tensioning drops (i.e. loss equal to 90% correspondent to Joint C), the gap opens at the beam-column interface. Consequently, the interstorey drift increases and the dissipaters (if present) are subjected to yielding. This implies that non-structural components (windows, facades, infills, etc.) may be subjected to damage with additional repair cost required. Furthermore, dissipaters that were subjected to plastic deformation should be replaced.

Concerning the Ultimate Limit State (ULS), results showed that when dissipaters are used the decrease in post-tensioning force does not significantly affect the displacement demand of the structure: the relative increment of drift respect to the initial condition is equal to 1%,1.9% and 8.6% for losses equal to 20%, 30% and 90%, respectively. This is due to both the damping ξ and the ductility μ of the system increasing at higher levels of post-tensioning loss as reported in Table 7.

The increase in ductility occurs because the gap opening happens at lower levels of moment demand, which reduces the amount of elastic deformation in the beam, column, and beam-column joint. This results in a higher rotation at the beam-column joint interface for the given total structural drift. This increase in rotation leads to higher strain in the dissipater going from 5% to 6.3% as shown Table 7. Greater damping lowers building accelerations and therefore lowers base shears.

In summary, the combination of post-tensioning and additional damping devices creates a situation where the loss of moment capacity from the post-tensioning is offset by an increase in hysteretic damping. This means that under the same input, a building with 0% or 90% loss will respond very similar in terms of maximum displacement. It should be noted however that if losses create a situation where the re-centring ratio decreases below approximately 0.55 (i.e. Joint C), the system will no longer re-centre (i.e. it will have residual displacements).

As shown in Figure 11 a significantly different situation can be observed from the ULS ADRS response of the structure without dissipaters. The post-tensioning force decrease causes a reduction in capacity, and without the additional hysteretic damping, the spectral demand remains unchanged and has a clear impact on building maximum drift. For a lower amount of post-tensioning loss (i.e within 30%), the drift increment is up to 9.7%, whereas for greater values (i.e. 90%), it reaches up to 37.4%. As the total moment capacity is provided by the post-tensioning only, there is no alteration in the re-centering capability of the structure as the post-tensioning force decreases.

Table 7: ADRS response for different levels of post tensioning loss respectively: nominal yielding displacement d_y, intersection displacement d_i, intersection acceleration a_i, maximum inter-storey drift dr_i, ductility μ, damping ξ, gap opening ϑ_g and strain in the dissipaters ε_{diss}.

Without dissipaters									
	Joint	**d_y [mm]**	**d_i [mm]**	**a_i [g]**	**dr_i [-]**	**Δdri [%]**	**μ [-]**	**ξ [-]**	**ε_{diss} [-]**
SLS	Initial	21.1	15.2	0.108	0.20%	0.0%	-	5.00%	-
	A	18.9	15.3	0.108	0.20%	0.6%	-	5.00%	-
	B	17.9	15.3	0.108	0.20%	0.9%	-	5.00%	-
	C	13.9	26.2	0.080	0.34%	69.1%	1.88	5.00%	-
ULS	Initial	21.1	185.2	0.201	2.01%	0.0%	8.78	5.00%	-
	A	18.9	196.9	0.188	2.13%	6.1%	10.4	5.00%	-
	B	17.9	204.4	0.183	2.20%	9.7%	11.4	5.00%	-
	C	13.9	254.6	0.146	2.76%	37.4%	18.3	5.00%	-
With Dissipaters									
	Joint	**d_y [mm]**	**d_i [mm]**	**a_i [g]**	**dr_i [-]**	**Δdri [%]**	**μ [-]**	**ξ [-]**	**ε_{diss} [-]**
SLS	Initial	33.4	25.3	0.180	0.32%	0.0%	-	5.00%	0
	A	31.2	25.4	0.180	0.32%	0.5%	-	5.00%	0
	B	30.2	25.4	0.180	0.32%	0.8%	-	5.00%	0
	C	20.5	29.8	0.163	0.38%	21.3%	-	5.00%	0
ULS	Initial	33.4	209.4	0.327	2.28%	0.0%	6.4	11.81%	5.0%
	A	31.2	211.9	0.312	2.30%	1.0%	6.9	13.01%	5.5%
	B	30.2	212.7	0.305	2.32%	1.9%	7.2	13.70%	5.6%
	C	20.5	226.6	0.264	2.48%	8.6%	11.4	17.60%	6.3%

Table 8: Ground motion selection for New Plymouth and Christchurch.

New Plymouth				**Christchurch**			
SLS		**ULS**		**SLS**		**ULS**	
Tag	**Name**	**Tag**	**Name**	**Tag**	**Name**	**Tag**	**Name**
22	El Alamo	20	Northern Calif-03	14	Kern County	179	Imperial Valley-06
70	San Fernando	179	Imperial Valley-06	22	El Alamo	182	Imperial Valley-06
336	Coalinga-01	415	Coalinga-05	122	Friuli, Italy-01	576	Taiwan SMART1(45)
722	Superstition Hills-02	570	Taiwan SMART1(45)	169	Imperial Valley-06	690	Whittier Narrows-01
840	Landers	759	Loma Prieta	573	Taiwan SMART1(45)	778	Loma Prieta
871	Landers	776	Loma Prieta	582	Taiwan SMART1(45)	808	Loma Prieta
1014	Northridge-01	787	Loma Prieta	871	Landers	1013	Northridge-01
1096	Northridge-01	821	Erzican, Turkey	916	Big Bear-01	1176	Kocaeli, Turkey
1215	Chi-Chi, Taiwan	1087	Northridge-01	1014	Northridge-01	1227	Chi-Chi, Taiwan
1277	Chi-Chi, Taiwan	1294	Chi-Chi, Taiwan	1181	Chi-Chi, Taiwan	1498	Chi-Chi, Taiwan

NON-LINEAR TIME HISTORY ANALYSIS (NLTH)

Although the ADRS method gives a good understanding of the dynamic behaviour of the structure, further investigation was carried out through NLTH analysis.

According to the modal analysis, the first natural period T is estimated to be equal to 0.85 s for both structures. The ground motions were selected from the NGA Database [34] and scaled according to NZS 1170.5 [1]. A performance factor S_p=1 was selected, and the scaling process was carried out minimizing the error between the ground motion and code spectra in the bandwidth between 0.4T and 1.3T. The record set is shown in Table 8, and their average spectra plotted in Figure 12 against the code spectrum.

Two sources of damping were considered in the model: viscous damping and hysteretic damping. Particular care has to be used in modelling viscous damping to avoid unintended consequences as pointed out by several authors (e.g. [35, 36]). In particular, several researches (e.g. [37-41]) showed that the Rayleigh damping formulation might lead to an overestimation of the internal forces and underestimation of displacements due to the arising of "spurious" damping forces. More appropriate formulations [42] are available in finite element software such as Ruaumoko [43] since the early '80s.

Recently, the possibility of constructing the global damping matrix by superimposing the model damping matrices [41] was introduced in Opensees [32]. Accordingly, this approach was implemented in this simulation.

Previous studies [44, 45] showed that the viscous damping in post-tensioned timber frames depends on the amount of drift expected, suggesting a value between 4% and 7% (without considering any partitions) for SLS and ULS, respectively.

A unique damping ratio equal to 5% was considered in this study, set in correspondence of the first eight elastic modes. Results are presented in Figure 13 and Figure 14 for the building without and with dissipaters, respectively. NLTH results confirmed what was identified by the ADRS analysis.

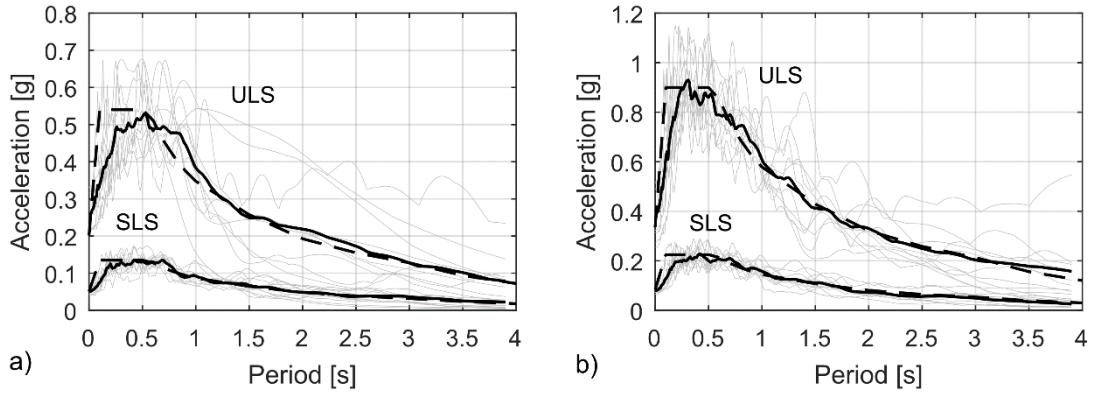

Figure 12: Average ground motions response compared with code spectrum for a) New Plymouth (New Zealand) and b) Christchurch (New Zealand) [1].

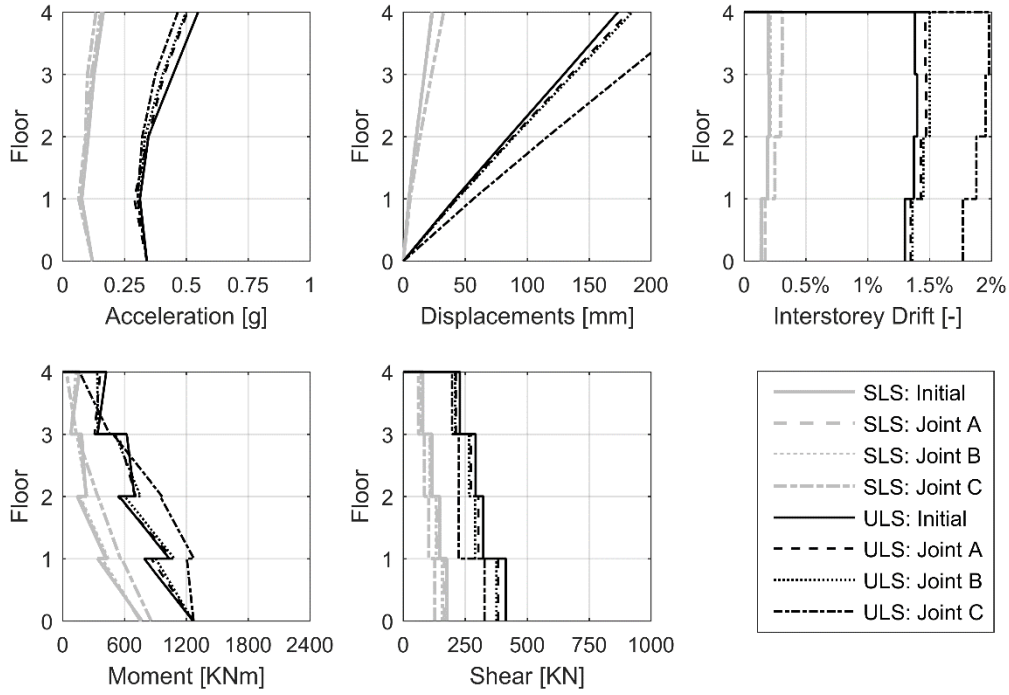

Figure 13: Non-Linear Time History Analysis results for the building without additional damping: a) floor acceleration, b) floor displacement, c) inter-storey drift, d) interstorey moment distribution and e) shear distribution.

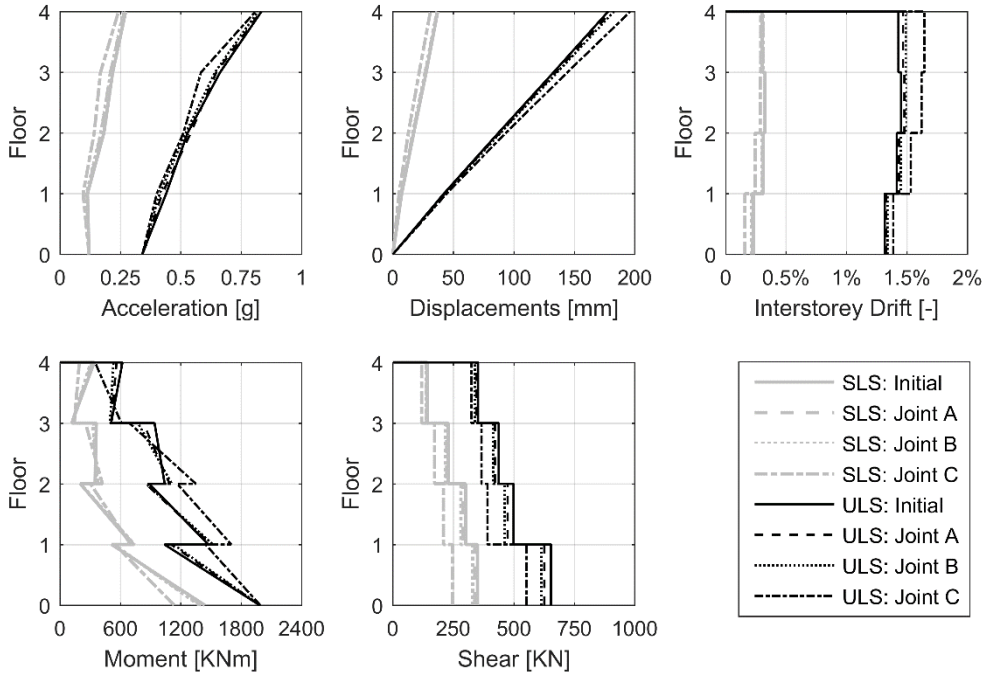

Figure 14: Non Linear Time History Analysis results for the building with additional damping: a) floor acceleration, b) floor displacement, c) inter-storey drift, d) interstorey moment distribution and e) shear distribution.

Regarding SLS, the two structures behaved similarly in terms of displacement, shear, acceleration, and moment profile when losses are within 30%. An increase of displacement and reduction of acceleration/forces can instead be observed when higher amount of losses take place (i.e. 90%). Again, this is due to the premature rocking activation.

At the ULS, the building without dissipaters (Figure 13) was subjected to greater displacements and inter-storey drifts when post-tensioning loss increases. As mentioned before, this is a result of the decrease in moment capacity. As dissipation is not provided, the spectrum remains unchanged causing greater displacements to the building. Another consequence is that the system was subjected to lower seismic force. In fact, floor accelerations, shear, and moment distributions decrease when post-tensioning loss increases.

When external dissipaters were provided (Figure 14), floor displacements and inter-storey drifts remained similar regardless post-tensioning loss. Again, this is due to the increase of energy dissipated (i.e. dissipaters are subjected to higher plastic demand) when the contribution of post-tensioning reduces. If displacements and inter-storey drift remain unchanged, floor accelerations, shear, and moment distribution are reduced as a consequence of higher dissipation when post-tensioning loss increases.

The top-floor displacement and the moment-rotation behaviour in correspondence of the gap interface (column at level 4) are presented in Figure 15a and b respectively for the Imperial Valley-06 ground motion (ID 179).. They represent the building with dissipaters at the initial condition and after 90% losses occurring (Joint C).

It can be noticed that the connection shows no complete re-centring when Joint C is adopted Figure 15b), and therefore small residual displacement occurs (Figure 15a).

As the re-centring capability depends on the ratio between post-tensioning and mild steel moments contribution, it decreases when losses increase allowing residual deformation.

It is worth to note however that the overall building re-centring property depends on the re-centring capability of each joint, including the base to column foundation: these are not affected by post-tensioning losses.

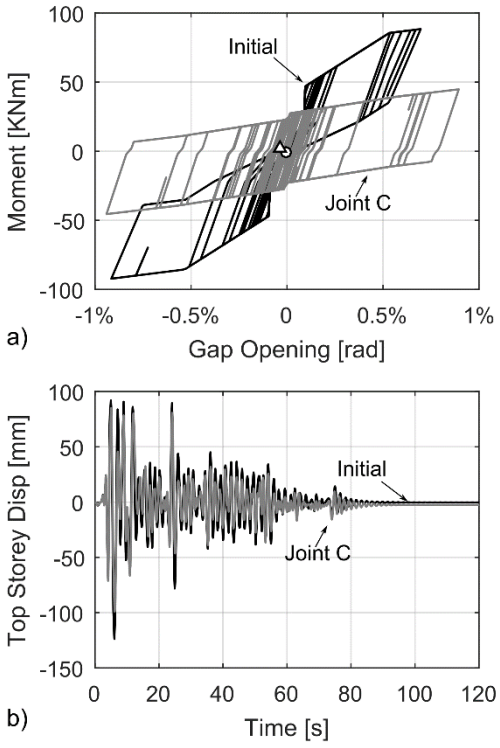

Figure 15: Building with dissipaters subjected to the Imperial Valley-06 ground motion (ID 179): a) First storey displacement over time: comparison between initial condition and Joint C response (i.e 90% of losses); b) moment-gap opening joint response: comparison between initial condition and Joint C behaviour. Circle and triangle represents the residual rotation point at the end of the ground motion.

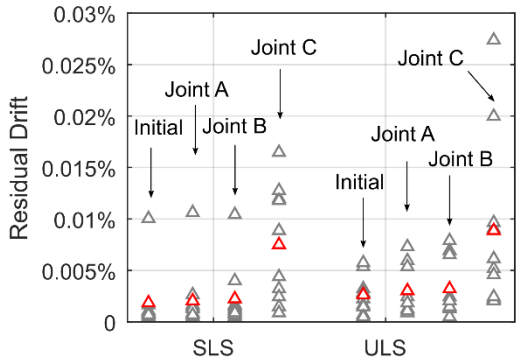

Figure 16: Residual drift in the building with additional damping (red triangles average values).

In this case, a decent re-centring can be observed despite losses occuring. This happens because the column-foundation joint was designed with a re-centring ratio of β equal to 0.7.

The re-centering joint capability of the only post-tensioned building instead is not affected by the amount of losses as the moment contribution given by post-tensioning is equal to the total moment. Therefore, β=1 is independent of the loss.

The residual drift for the building with additional damping is presented in Figure 16. It can be noticed that the performance at SLS is almost equal except for joint C, where the average residual increase doubled. Similarly, at the ULS, the residual drift slightly increased when post-tensioning loss stayed within 30% before doubling for loss values equal to 90%.

In conclusion, the building re-centering capability depends on the post-tensioning (or gravity)/mild steel moment contribution ratio: if the overall ratio stays above 0.55-0.5, significant residual deformations should not occur.

CONCLUSION

Post-tensioning losses have been always considered a crucial aspect that affects the in-time seismic behaviour of Pres-Lam frames. The different levels of detailing in the beam-column joints can result in a huge variation of post-tensioning losses. Hardwood reinforcement (Joint A) and steel armouring (Joint B) lead to 20 and 30% losses respectively within 50 years. If no precautions are taken to protect the joint, the amount of loss may dramatically increase (Joint C).

The outcomes of the numerical analyses supported by monitored data addressed important aspects, which range from the individual connection up to the overall system level:

1. Push-pull analysis results showed that post-tensioning loss decreases the total moment capacity of the building and causes the gap opening to occur at a lower level of moment demand. The area enclosed in the moment-rotation loop however remains unchanged regardless of the post-tensioning loss as it depends only on the steel contribution (if present). Furthermore, higher levels of post-tensioning loss (i.e. 90%) affect the re-centring capability of the hybrid joint by introducing a residual deformation.
2. At building level, both the ADRS and the NLTH analysis results showed that when dissipaters are used, the building is subjected to similar displacements regardless of the amount of post-tensioning loss at the ULS. The loss of moment capacity is in fact balanced by the increase of damping due to the early activation of dissipaters, which results in higher ductility and damping values. As dissipaters are subjected to higher plastic demand, the unbounded length should be slightly increased in the design phase to accommodate for the extra amount of deformation when significant losses are expected.
3. Conversely, if dissipaters are not provided, the building is subjected to greater inter-storey drift as post-tensioning losses occur. Since the moment capacity is entirely provided by post-tensioning and no further damping is present, floor displacements increase with post-tensioning loss increase. This extra amount of displacement is limited when losses are within 30%, but greater losses may compromise the structural safety.
4. If supplemental dissipation is provided or not, post-tensioning loss might affect the SLS performance of the building. While the effect of 20%-30% losses is almost negligible, the early rocking activation due to excessive losses (i.e. 90%) might cause unintended damage to no-structural elements by increasing the interstorey drift. In terms of serviceability, this would introduce further reparability costs.

Overall, design solutions such as armouring the columns (Joint B) or adopting hardwood (Joint A) are proving to contain the losses within a limited amount (i.e. 30% in 50 years). In this scenario, the rocking motion is therefore activated only for rare events, and the building serviceability can be preserved for likely earthquakes during the entire building life.

Design Recommendations

As the scope of this paper was limited to only two case studies, further research is needed to obtain a more comprehensive overview of the problem. Nevertheless, some recommendations are proposed.

The use of additional dissipation devices provides the building with further redundancy against rare and strong earthquakes (ULS), mitigating the effect of post-tensioning losses. However, it does not provide any benefits in terms of serviceability requirement (SLS).

Their use is therefore suggested whenever scenarios of losses equal to 30-40% might dramatically affect the building ULS displacement and/or when additional moment capacity is necessary to accommodate the seismic demand.

ACKNOWLEDGEMENTS

The authors would like to acknowledge Mr. Paul Drummod for providing the data from the Trimble Navigation Office and Claude Leyder for providing the data from the House of Natural Resources. The authors would also like to thank Professor Athol Carr for his suggestions and knowledge regarding damping models.

REFERENCES

1. Standard NZ (2004). "*NZS 1170.5: Structural Design Actions- Earthquake Actions, New Zealand*". Wellington, New Zealand.
2. Priestley NMJ (1996). "The PRESS program - Current status and proposed plans for phase III". *PCI Journal*, **4**(2): 22-40.
3. Priestley NMJ (1991). "Overview of the PRESSS Research Program". *PCI Journal*, **36**(4): 50-57.
4. Christopoulos C, Filiatrault A, Uang C and Folz B (2002). "Post-Tensioned Energy Dissipating Connections for Moment Resisting Steel Frames". *ASCE Journal of Structural Engineering*, **128**(9): 1111-1120.
5. Palermo A, Pampanin S, Buchanan A and Newcombe M (2005). "Seismic design of multi-storey buildings using laminated veneer lumber (LVL)". *New Zealand Society for*

Earthquake Engineering Conference, Wairakei, New Zealand.

6. Buchanan A, Deam B, Fragiacomo M, Pampanin S and Palermo A (2008). "Multi-storey prestressed timber buildings in New Zealand". *Structural Engineering International: Journal of the International Association for Bridge and Structural Engineering (IABSE)*, **18**(2): 166-173.
7. Newcombe M, Pampanin S and Buchanan A (2010). "Global response of a two storey Press-Lam timber building". *New Zealand Society for Earthquake Engineering Annual Conference*, Wellington, NZ, Paper no 28.
8. Sarti F, Palermo A and Pampanin S (2015). "Quasi-Static Cyclic Testing of Two-Thirds Scale Unbonded Posttensioned Rocking Dissipative Timber Walls". *ASCE Journal of Structural Engineering*, **142**(4): 1-14.
9. Smith T, Pampanin S, Carradine D, Buchanan A, Ponzo F, Cesare A and Nigro D (2011). "Experimental investigations into post-tensioned timber frames with advanced damping systems". *Proceedings of Il XIV Convegno di Ingegneria Sismica, Associazione Nazionale di Ingegneria Sismica*, Bari, Italy.
10. Dumbar A, Pampanin S, Palermo A and Buchanan A (2014). "Seismic design of core-walls for multi-storey timber buildings". *New Zealand Society for Earthquake Engineering Conference*; Wellington, New Zealand.
11. Iqbal A, Pampanin S and Buchanan AH (2016). "Seismic Performance of Full-Scale Post-Tensioned Timber Beam-Column Connections". *Journal of Earthquake Engineering*, **20**(3): 383-405.
12. Wanninger F and Frangi A (2014). "Experimental and Analytical Analysis of a Post-Tensioned Timber Connection Under Gravity Loads". *Engineering Structures*, **70**: 117-29.
13. Di Cesare A, Ponzo FC, Simonetti M, Smith T and Pampanin S (2013). "Numerical modeling of a post-tensioned timber frame building with hysteretic energy dissipation". *International Conference on Structural Engineering, Mechanics and Computation*, Cape Town, South Africa.
14. Davies M and Fragiacomo M (2011). "Long-Term Behavior of Prestressed LVL Members. I: Experimental Tests". *ASCE Journal of Structural Engineering*, **137**(12): 1553-61.
15. Fragiacomo M and Davies M (2011). "Long-Term Behavior of Prestressed LVL Members. II: Analytical Approach". *ASCE Journal of Structural Engineering*, **137**(12): 1562-72.
16. Wanninger F, Frangi A and Fragiacomo M (2014). "Long Term Behavior of Poste Tensioned Timber Connections". *ASCE Journal of Structural Engineering*, **141**(6): 04014155.
17. Wanninger F and Frangi A (2014). "Experimental Analysis of a Post-Tensioned Timber Connection". *Materials and Joints in Timber Structures*, Springer, Heidelberg, 57-66p. (https://www.springer.com/us/book/9789400778108).
18. Leyder C, Wanninger F, Frangi A and Chatzi E (2014). "Field Testing on Innovative Timber Structures". *World Conference on Timber Engineering*; Quebec City, Canada.
19. Brown A, Lester J and Pampanin S (2014). "Re-building Trimble Navigation's Office Using a Damage-limiting Seismic System". *World Conference on Timber Engineering*; Quebec City, Canada.
20. Sarti F, Palermo A and Pampanin S (2016). "Fuse-Type External Replaceable Dissipaters: Experimental Program and Numerical Modeling". *ASCE Journal of Structural Engineering*, **142**(12): 04016134.
21. Drummond P, Lester J and Ruffin P (2014). " *Trimble New Zealand: New Offices Rebuilt to a Higher Standard of Seismic Resilience*". White Paper: Trimble Navigation.
22. Smith T et al. (2016). "Long Term Dynamic Characteristics of a PresLam Structure". *World Conference on Timber Engineering*; Vienna, Austria.
23. Granello G, Leyder C, Palermo A, Frangi A and Pampanin S (2017). "Design Equations to Predict Losses in Post-Tensioned Timber Structures". *International Meeting on Timber Engineering Research*; Kyoto, Japan.
24. Leyder C, Chatzi E and Frangi A (2015). "Structural Health Monitoring of an Innovative Timber Building". *International Conference on Performance-based and Life-Cycle Structural Engineering*; Brisbane, Australia.
25. Newcombe MP, Pampanin S and Buchanan AH (2010). "Experimental Testing of a Two-Storey Post-Tensioned Timber Building". *Canadian Conference on Earthquake Engineering*.
26. Carradine D et al. (2012). "Study of a high performance timber building: Design, construction and performance". *World Conference on Timber Engineering*, **2**: 253-261.
27. Yeoh D and Carradine D (2012). "*Long-Term Monitoring in Expan Building*". STIC Research Report, University of Canterbury, Christchurch, NZ.
28. Palermo A (2004). "*Use of Controlled Rocking in the Seismic Design of Bridges"*. PhD Thesis, Technical University of Milan, Milan, Italy.
29. Newcombe MP, Pampanin S, Buchanan A and Palermo A (2008). "Section Analysis and Cyclic Behavior of Post-Tensioned Jointed Ductile Connections for Multi-Story Timber Buildings". *Journal of Earthquake Engineering*, **12**(Sup1): 83-110.
30. Smith T (2014). "*Post-tensioned Timber Frames with Supplemental Damping Devices"*. PhD Thesis, University of Canterbury, Christchurch, NZ.
31. Chopra AK and Rakesh KG (1999). "Capacity-Demand-Diagram Methods based on Inelastic Design Spectrum". *Earthquake Spectra*, **4**(15).
32. McKenna F, Fenves GL and Scott MH (2000). "Open System for Earthquake Engineering Simulation". *University of California, Berkely, CA*.
33. Pampanin S, Palermo A and Buchanan A (2013). "*Post-Tensioned Timber buildings - Design Guide Australia and New Zealand*". Structural Timber Innovation Company, Christchurch, NZ.
34. Chiou B, Darragh R, Gregor N and Silva W (2008). "NGA project strong-motion database". *Earthquake Spectra*, **24**(1): 23-44.
35. Charney FA (2008). "Unintended Consequences of Modeling Damping in Structures". *Journal of Structural Engineering*, **134**(4): 581-92.
36. Hall JF (2006). "Problems encountered from the use (or misuse) of Rayleigh damping". *Earthquake Engineering and Structural Dynamics*, **35**: 522-45.
37. Crisp DJ (1980). "*Damping Models for Inelastic Structures"*. Master Thesis: University of Canterbury; Christchurch, NZ.
38. Bernal D (1994). "Viscous Damping in inelastic structural response". *ASCE Journal of Structural Engineering*, **120**(4): 1240-1254.
39. Carr AJ (1997). "Damping Models for Inelastic Structures". *Asia Pacific Vibration Conference*; Kyongju, Korea.

40. Carr AJ (2005). "Damping Models for Time-history Structural Analyses". *Asia Pacific Vibration Conference*, Langkawi, Malaysia.

41. Chopra AK and McKenna F (2016). "Modeling viscous damping in nonlinear response history analysis of buildings for earthquake excitation". *Earthquake Engineering and Structural Dynamics*, **45**(2): 193-211.

42. Wilson E and Penzien J (1972). "Evaluation of orthogonal damping matrices". *International Journal for Numerical Methods in Engineering*, **4**(1): 5-10.

43. Carr AJ (2007). "*Ruaumoko Manual-Theory*". University of Canterbury, Christchurch, NZ.

44. Pino Merino D (2011). "*Dynamic Response of Post-Tensioned Timber Frame Buildings"*. Master Thesis, University of Canterbury, Christchurch, NZ.

45. Newcombe MP (2011). "*Lateral Force Design of Post-Tensioned Frame and Wall Buildings"*. PhD Thesis, University of Canterbury, Christchurch, NZ.